Computational model of carbachol-induced δ, θ and γ-like oscillations in hippocampus☆

J.-M. Fellous[a], P.H.E. Tiesinga[a,*], J.V. José[b], T.J. Sejnowski[a]

[a]*Sloan Center for Theoretical Neurobiology and Computational Neurobiology Laboratory, The Salk Institute, 10010 N. Torrey Pines Rd, La Jolla, CA 92037, USA*
[b]*Center for Interdisciplinary Research on Complex Systems, and Department of Physics, Northeastern University, Boston, MA 02115, USA*

Abstract

Application of carbachol (cch) can induce oscillations in the δ (cch-δ, 0.5–2 Hz), θ (cch-θ, 4–12 Hz), and γ (cch-γ, 30–80 Hz) frequency-range in the rat hippocampal slice preparation. Using model CA3 cells we found that the time scale for cch-δ was determined by the decay constant of $I_{K\text{-AHP}}$, that of cch-θ by an intrinsic subthreshold membrane potential oscillation, and that of cch-γ by the decay constant of GABA-ergic postsynaptic potentials. The known physiological effects of carbachol on I_M and $I_{K\text{-AHP}}$, and on the strength of excitatory postsynaptic potentials produced the observed transitions from incoherent cch-θ to cch-δ, and from cch-δ to cch-θ with increasing cch concentrations, as well as the nested cch-γ-δ and cch-γ-θ seen in experiment. © 2001 Elsevier Science B.V. All rights reserved.

Keywords: Oscillation; Neuromodulator; Synchrony; Biophysical model

1. Introduction

Multiple rhythms recorded from the human brain reflect the spatially and temporally coherent activity of large populations of cells. In this paper we focus on three bands of oscillations that have been found during animal behavior and in human

Table 1
Parameter values for the pyramidal cell model for low, medium, and high carbachol concentrations[a]

	cch (μM)	g_{Ca}	g_{K-AHP}	g_M	g_{AMPA} (%)
Low	1–4	10	0.8	0.3–0.4	100
Medium	4–13	10	0.8	0.2–0.3	100
High	13–40	6	0.2	0.0	50

[a]Conductances are in mS/cm^2.

electroencephalograms (EEGs): δ (0.5–2 Hz), θ (5–12 Hz) and γ (30–80 Hz). How can neuronal networks generate oscillatory activity in these widely different frequency ranges? How does the brain control which frequencies are expressed?

Here we address these issues in a model study of rhythmogenesis in the hippocampal slice. In vitro muscarinic activation of rat hippocampal area CA3 produces synchronous population activity in these frequency bands [1–4,7,13]. The level of activation of cholinergic receptors determines which of the three oscillations will occur or predominate [3]. The goal of the present study is to offer parsimonious, experimentally testable hypotheses explaining the presence of δ, θ and γ-like rhythms in the CA$_3$ field of the hippocampus. These hypotheses rely on the known cellular and synaptic effects of carbachol, and further allow for the understanding of the transitions between these different rhythms.

2. Methods

The CA3 model network consisted of 500 pyramidal cells and 100 interneurons. Pyramidal cells projected to other pyramidal cells and interneurons via AMPA synapses, the interneurons projected to other interneurons and pyramidal cells via GABA$_A$ synapses. The pyramidal cells were sparsely connected with a probability $p = 0.1$–0.5. The interneurons were connected all to all. The pyramidal to interneuron, and vice versa, connection probabilities were free parameters in our study. We used a modified Pinsky–Rinzel model [10,11] to describe the pyramidal cells. Each cell consisted of two compartments, containing the Hodgkin–Huxley spike-generating (I_{Na} and I_{K-DR}), leak (I_L), calcium (I_{Ca}), calcium-dependent potassium (I_{K-C} and I_{K-AHP}), and muscarinic potassium (I_M) currents. We also added persistent-like sodium I_{NaO} and potassium I_{KO} currents, that are responsible for θ-frequency subthreshold membrane potential oscillations [6]. Carbachol blocked in a dose dependent manner I_{K-AHP}, I_M and I_{Ca} [8,9] and it depressed synaptic transmission [5]. To account for these effects we divided the carbachol concentration in three regimes, low, medium, and high concentration. The parameter settings were based on Refs. [5,8,9] and are listed in Table 1.

The interneuron model was taken from Ref. [12]. The depolarizing effects of carbachol on the interneuron were modeled as an injected current. A detailed description of the model and its implementation is given elsewhere [11].

3. Results

We first summarize the experimental results [3]. For low carbachol concentrations intracellular recordings show subthreshold membrane potential oscillations with spikes during some cycles. Concurrent recordings of the field potential do not show synchronous θ frequency activity. Hence the neurons fire independently from each other. This state is called asynchronous or incoherent cch-θ. For medium carbachol concentrations synchronous population activity at 0.5–2 Hz (cch-δ) was present in the field potential. The pyramidal cells fired multiple spikes or sometimes bursts during these population events. At high cch concentrations synchronous activity in the θ frequency range (cch-θ) was present in the field potential. Some pyramidal cells fired on all cycles, other cells missed cycles. For cch concentrations between 8 and 40 µM synchronous γ oscillations were sometimes observed in combination with cch-δ or cch-θ.

Our model reproduced the above experimental results. Specifically, we find asynchronous cch-θ for low, cch-δ for medium, and cch-θ for high carbachol concentrations. We also obtain cch-γ interspersed with cch-δ and cch-θ for medium and high concentrations, respectively. The transitions from asynchronous cch-θ to cch-δ to cch-θ were also simulated by gradually changing the values of the parameters from one cch regime to the other (Table 1). These results are described in more detail elsewhere [11].

cch-δ. The cch-δ oscillation proceeds in four steps, as indicated by the numbers in Fig. 1A. A population burst is initiated only when a critical number of neurons fire at approximately the same time. This number defines a threshold for the time-dependent firing rate. (1) At a certain time, a spontaneous fluctuation brings the network activity above threshold. The probability for this to occur depends on the excitability of the neurons, it is partly regulated by the magnitude of I_M. (2) The above threshold activity recruits more and more neurons in an 'explosive' process. The speed with which the activity spreads through the network depends on the unitary conductance g_{AMPA} of the recurrent excitation and probability P_{ee} of a synapse between two neurons. (3) The slow after hyperpolarization (AHP) current is activated by action potential generation. When this hyperpolarization reaches a certain value the neuron becomes refractive. The population event is terminated when more and more neurons become refractive. The details of this process depend on the interplay of I_{Ca} and $I_{K\text{-}AHP}$. (4) The slow AHP then slowly decays, during which time there is little or no spiking activity. The duration of this silent phase depends on the decay constant $t_{K\text{-}AHP}$. The oscillation frequency of cch-δ is plotted as a function of $t_{K\text{-}AHP}$ in Fig. 2A. For the initiation of the population event I_M should be small enough, and g_{AMPA} and P_{ee} large enough. Hence blocking AMPA synapses, or decreasing carbachol concentration would terminate the oscillations. For the population event to terminate I_{Ca} and $I_{K\text{-}AHP}$ should be strong enough. In our simulations we typically find an asynchronous activity state (or cch-θ) when reducing $I_{K\text{-}AHP}$.

cch-θ: During cch-θ (Fig. 1B) one group of neurons (1) is depolarized and fires in the θ-frequency range, and the other group (2) is less depolarized and is subthreshold. The discharge of group 1 is synchronized by the recurrent excitation. The subthreshold
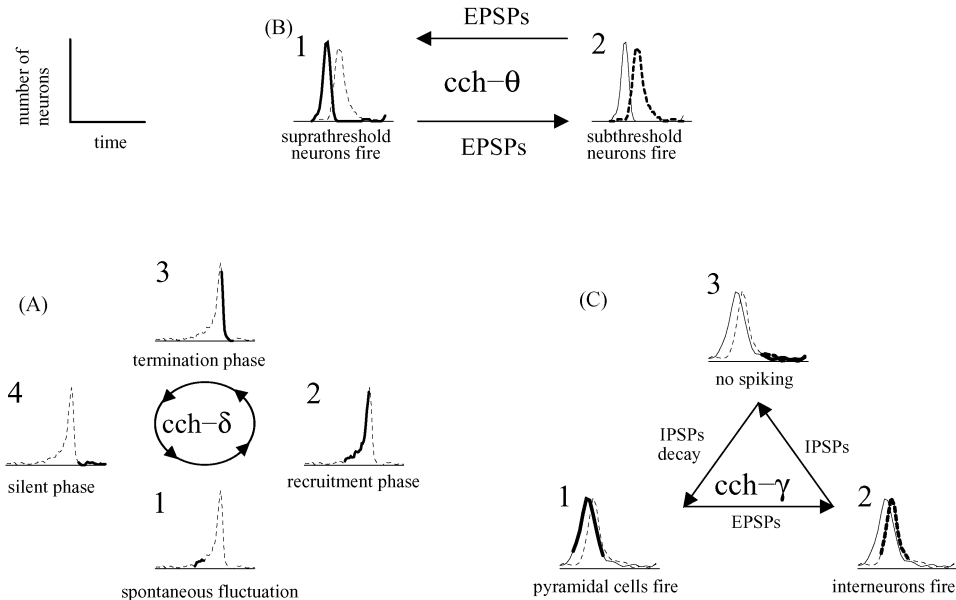
Fig. 1. Mechanisms for (A) cch-δ, (B) cch-θ and (C) cch-γ. In each panel we plot the firing-rate histogram of the network neurons as a function of time for one cycle of the oscillation. The same histogram is repeated four (A), two (B) and three (C) times for consecutive stages of the oscillation, as indicated by the number in the left-hand side corner of each graph. The network activity during that period is highlighted by a fat curve on top of the histogram. The network neurons participating in the oscillation are (A) pyramidal cells (dashed line); (B) above threshold (solid line) and below threshold (dashed line) pyramidal cells; (C) interneurons (dashed line) and pyramidal cells (solid line). Time and firing rate are in arbitrary units. See the main text for a complete description of each mechanism.

neurons in the second group resonate to the synchronous synaptic drive generated by the first group, generating spikes on some of the cycles. The spikes are therefore in synchrony with the field potential, and they generate a weak depolarization in group 1 neurons. The level of depolarization generated by an injected current I_e determines the firing rate of the depolarized neurons. The dependence of the network oscillation frequency and its coherence on I_e is shown Fig. 2B. Due to the interaction with the subthreshold membrane oscillation, the network only discharges coherently in the θ-frequency range, despite the fact that individual neurons can spike at higher rates.

cch-γ: The cch-γ oscillation consists of three phases, as depicted in Fig. 1C. (1) First pyramidal cells fire. The resulting excitatory activity recruits more pyramidal cells and (2) interneurons. The interneuron activity generates an inhibitory synaptic drive that (3) stops the pyramidal cell and interneuron discharge. The pyramidal cell activity resumes when the inhibition has sufficiently decayed. The period of the oscillation is determined by the decay time t_{GABA} of the inhibitory synapses onto pyramidal cells, this was confirmed by simulations (Fig. 2C). The model predicts that blocking either
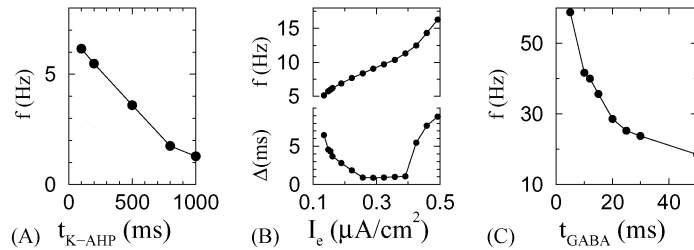
Fig. 2. Oscillation frequencies of (A) cch-δ as a function of $t_{K\text{-}AHP}$, (B) cch-θ as a function of I_e and (C) cch-γ as a function of t_{GABA}. In (B, bottom) the average dispersion $\varDelta$ of the spike times during one oscillation cycle is plotted. See text for details.

GABA$_A$ or AMPA synapses will abolish the oscillations, as was observed experimentally [4].

4. Discussion

The models studied here show how spatially diffuse cholinergic modulation may influence the temporal dynamics of the CA$_3$ region of the hippocampus. Through effects of carbachol on specific intrinsic and synaptic currents, this modulation is able to bias the same anatomical circuitry into operating in four distinct dynamical modes corresponding to EEG states observed in vivo. The model makes predictions that can be tested by experimental manipulation of cholinergic levels in vitro and in vivo during behavioral tasks.

References

[1] B.H. Bland, L.V. Colom, J. Konopacki, S.H. Roth, Intracellular records of carbachol-induced theta rhythm in hippocampal slices, Brain Res. 447 (1988) 364–368.

[2] C.T. Dickson, G. Biella, M. de Curtis, Evidence for spatial modules mediated by temporal synchronization of carbachol-induced γ rhythm in medial entorhinal cortex, J. Neurosci. 20 (2000) 7846–7854.

[3] J.-M. Fellous, T.J. Sejnowski, Cholinergic induction of oscillations in the hippocampal slice in the slow (0.5–2 Hz), θ (5–12 Hz) and γ (35–70 Hz) bands, Hippocampus 10 (2000) 187–197.

[4] A. Fisahn, F.G. Pike, E.H. Buhl, O. Paulsen, Cholinergic induction of network oscillations at 40 Hz in the hippocampus in vitro, Nature 394 (1998) 186–189.

[5] M.E. Hasselmo, E. Schnell, Laminar selectivity of the cholinergic suppression of synaptic transmission in rat hippocampal region CA1: computational modeling and brain slice physiology, J. Neurosci. 14 (1994) 3898–3914.

[6] L.W. Leung, C.Y. Yim, Intrinsic membrane potential oscillations in hippocampal neurons in vitro, Brain Res. 553 (1991) 261–274.

[7] B.A. MacVicar, F.W. Tse, Local neuronal circuitry underlying cholinergic rhythmical slow activity in CA$_3$ area of rat hippocampal slice, J. Physiol. (Lond.) 417 (1989) 197–212.

[8] D.V. Madison, B. Lancaster, R.A. Nicoll, Voltage clamp analysis of cholinergic action in the hippocampus, J. Neurosci. 7 (1987) 733–741.

[9] E.D. Menschik, L.H. Finkel, Cholinergic neuromodulation and Alzheimer's disease: from single cells to network simulations, Progr. Brain Res. 121 (1999) 19–45.

[10] P.F. Pinsky, J. Rinzel, Intrinsic and network rhythmogenesis in a reduced Traub model for CA_3 neurons, J. Comput. Neurosci. 1 (1994) 39–60.

[11] P.H.E. Tiesinga, J.-M. Fellous, J.V. José, T.J. Sejnowski, Computational model of carbachol-induced δ, θ and γ oscillations in the hippocampus, Hippocampus (2001). In press.

[12] X.J. Wang, G Buzsáki, Gamma oscillation by synaptic inhibition in a hippocampal interneuronal network model, J. Neurosci. 16 (1996) 6402–6413.

[13] J.H. Williams, J.A. Kauer, Properties of carbachol-induced oscillatory activity in rat hippocampus, J. Neurophysiol. 78 (1997) 2631–2640.

Jean-Marc Fellous did his undergraduate studies in Marseille, France. Graduate studies included a Master's degree in artificial intelligence (Paris VI University, France), and Ph.D. in Computer Science with an emphasis on brain theory and neural networks at the University of Southern California, Los Angeles. Postdoctoral studies included slice neurophysiology and neural modeling in the laboratories of John Lisman (Brandeis University) and Terrence Sejnowski (Salk Institute). Jean-Marc Fellous is currently a Howard Hughes Institute Research Associate in the computational neurobiology laboratory. His interests include the computational roles of neuromodulation and rhythmogenesis.

Paul Tiesinga studied Theoretical Physics at Utrecht University in the Netherlands. His Ph.D. thesis was on the dynamics of Josephson-junction arrays. As a postdoctoral fellow at Northeastern University he worked on biophysically realistic modeling of thalamus and hippocampus. Currently he is a Sloan Fellow at the Salk institute in La Jolla.

Jorge José studied at the National University of Mexico in the field of theoretical condensed matter physics. He has held positions at Brown University, University of Chicago, University of Mexico, and University of Utrecht (The Netherlands). Currently he is the Matthews Distinguished University Professor and the Director of the Center for Interdisciplinary Research on Complex Systems at Northeastern University. He is a Corresponding Member of the Mexican National Academy of Sciences. He is presently interested in synchronization and noise in neural network systems.

Terrence Sejnowski is an Investigator with Howard Hughes Medical Institute and a Professor at the Salk Institute for Biological Studies where he directs the Computational Neurobiology Laboratory. He is also Professor of Biology at the University of California, San Diego, where he is Director of the Institute for Neural Computation. Dr. Sejnowski received a B.S. in physics from the Case-Western Reserve University, a M.A. in physics from Princeton University, and a Ph.D. in physics from Princeton University in 1978. In 1988, Dr. Sejnowski founded Neural Computation, published by the MIT press. The long-range goal of Dr. Sejnowski's research is to build linking principles from brain to behavior using computational models.